

Ph.D. Showcase: Measuring Terrain Distances Through Extracted Channel Networks

PhD Student:
Christopher Stuetzle
Dept. Computer Science
stuetc@cs.rpi.edu

PhD Supervisor:
W. Randolph Franklin
Dept. Electrical Engineering
wrf@ecse.rpi.edu

PhD Supervisor:
Barbara Cutler
Dept. Computer Science
cutler@cs.rpi.edu

Mehrad Kamalzare
Dept. Civil Engineering
kamalm@rpi.edu

Zhongxian Chen
Dept. Computer Science
chenz5@cs.rpi.edu

Thomas Zimmie
Dept. Civil Engineering
zimmit@rpi.edu

ABSTRACT

This paper initiates a forensic analysis of the causes of levee failures by analyzing and extracting information from a sequence of elevation data. This is a crucial step in bettering the design and construction of levees and dams. (Fully diagnosing failures usually requires knowledge beyond the geometry of the levee, such as weather conditions and material properties). We use results from computer simulations of levee overtopping for training data. The simulations use smoothed particle hydrodynamics coupled with a well-known erodibility model. Using the sequential nature of our data, we extract important channel networks that form as the soil is scoured away. We present a series of metrics to measure the distance between channel networks to assist in determining the critical threshold value used to extract important channels from the flow network. Methods for determining this “ideal” threshold have gone mainly unexplored, and so we present a comparison of various threshold values and how closely they identify matching channel networks on sequential terrains. These threshold values allow us to identify important properties of the terrain that form its “fingerprint”, a way of characterizing the geometry of the terrain. Our method for fingerprinting terrain is an important step toward the diagnosis of levee failure from digital elevation data.

Categories and Subject Descriptors

I.3.5 [Computer Graphics]: Computational Geometry and Object Modeling—*physically based modeling*;

I.6.4 [Simulation and Modeling]: Model Validation and Analysis *and* Simulation Output Analysis

Keywords

river network extraction, shape analysis

1. INTRODUCTION

Forensic analysis of the cause of levee failures continues to be critical in assessing levee construction and safety, and

its automation would make this necessary process faster and cheaper. After a catastrophe involving levee breach, such as the tragedy in New Orleans during Hurricane Katrina, civil engineers attempt to piece together the causes of the failure, usually seepage and/or overtopping [19].

We aim to automate this diagnostic process by performing a detailed analysis of the levee geometry, represented as one or more a Digital Elevation Models (DEMs). Toward this goal, we present a framework for detailed comparison of eroded terrains that introduces the notion of terrain distance, combining channel network and terrain characteristic distance metrics. Given a sequence of temporally connected terrains, we wish to minimize the difference between sequential terrains. This would allow for closer analysis of the erosion process, and so a method for minimizing the distance between two terrains, with regard to the characteristics that define them, is essential.

1.1 Channel Networks

An important characteristic of a terrain is the drainage, or channel, network, because hydraulic erosion is a prime factor in the formation of terrain geometry, particularly for levee breach events that motivate our work. Accurate and efficient extraction of these networks from DEM heightfield data has been an area of study for several decades ([16], [1], etc.). It is essential for the analysis and comparison of terrains as it allows for identification of channels, watersheds, valleys, and drainage basins, but its challenges stem from the fact that the data contains no information regarding the behavior of basins.

O’Callaghan and Mark [16] were among the first to extract a channel network from a DEM. For each pixel of the terrain, the direction of the lowest of its eight neighbors is set as the flow direction. The pixels are sorted by elevation, and flow accumulation is calculated. The authors apply a threshold to the flow values, allowing the extraction of pixels belonging to the channel network. This practice is widely used in channel network extraction, and finding the best threshold for a particular terrain is a specific objective of our work. Slight variations in geometry could render a threshold significantly less useful, and so when dealing with sequential data an adaptive threshold is vital. Comparing two terrains only makes sense if they have similar channel networks, and so identifying the thresholds that minimize the difference

between the extracted networks is a fundamental research question.

L. Band [1] describe a method for extending O’Callaghan and Mark’s work to identify channel watersheds by grouping pixels that flow into the same channel together. Once grouped, they can act as a single pixel and can accumulate flow as one, thus minimizing the need for tie breaking. However, this does not solve the problem of flat basins completely. Yang et al. [22] describe the effect various thresholds have on two widely used watershed analysis tools, the *width function* and the *area function*, finding that at low thresholds the two measures are similar but vary greatly as thresholds increase and channel networks shrink. Montgomery and Foufoula, in [15] present a comparison between the constant threshold and slope-dependent models for calculating drainage networks, presenting the conclusion that each method appears valid in certain instances. They also describe a method for identifying channel heads as a means for extracting channels.

Other methods for channel network extraction have required additional input. Turcotte et al. [21] introduce the *Digital River and Lake Network*, which is required as input in addition to a DEM. This allows for the handling of lakes in the terrain, a source of frustration for previous methods because of the difficulty of tie-breaking procedures and the lake of flow volume. Some methods have foregone flow calculation entirely and depended upon the geometry of the terrain surface exclusively, such as Lashermes et al. [10], who present a method for extracting valleys and hills from a terrain using wavelet filtering on high resolution DEMs. Still other methods have attempted to define characteristics on the terrain. Kramer and Marder [9] use a shallow water simulation to model the flow of water over the terrain, measuring the formation of channels with the area and width functions. Similarly, Soille et al. [20] overcome the tie-breaking dilemma in network extraction by running a flooding simulation to create a path through pits in the terrain. However, in both of these methods computation costs make analysis of large terrains difficult.

In our work, flow field calculation is a black box process, allowing substitution of different methods for calculation of the flow field and direction field. For this work, we use a variation of the least-cost flow routing method by Metz et al. [14]. For any pixel on the terrain, the least-cost path off of the edge of the terrain is calculated, and that determines the direction of flow. This method robustly minimizes the tie-breaking dilemma that arises when calculating flow direction in large, flat basins, and scales well to very large terrains.

1.2 Analysis of Shapes

Shape analysis has been studied in computer graphics and computer vision for decades, most often used in shape matching and pattern recognition. Shape matching is the process of choosing from a set of possible partners the closest to a given shape, while pattern recognition is a computer vision problem involving picking out examples of a given shape in an image or scene. Shape matching relies on difference metrics, measures of the dissimilarity between two shapes. The smaller the dissimilarity, the closer the two shapes are to one another.

Treating terrains and their associated channel networks as shapes is a method for comparison from which distance metrics arise naturally. Fundamentally we wish to be able

to compare the shapes of the channel networks that are extracted from terrain data.

Often, shape dissimilarity metrics are used as bases for finding the correlation between shapes, if one exists. Belongie et al. [2] present the idea of “Shape Contexts“, in which a two dimensional shape is described by the angle to the X-axis of every point along the shape’s border. In this instance, the X_2 metric can be used as the dissimilarity measure between the shapes. An extension [3] to this idea broadens the criteria for the shape context by basing its measure on the shape’s angle relative to the tangent along the shape border instead of the X-axis, making the shape context operation invariant under rotation.

Shape comparison was later applied to three dimensions by Osada [17], who presents the idea of representing three dimensional shapes as a probability distribution. Given any shape distribution function (such as the $D2$ function, a measure of Euclidean distance between two random points on the shape surface), they build a probability distribution function of the shape by selecting random points along the surface. These probability distributions can then be compared and analyzed by any known means.

Roy et al. [18] provide a metric for comparing triangle meshes. For each sampled point on the first mesh and a given shape attribute, the method finds the closest point of the same attribute in the comparison mesh. Geiger et al. [6] find the Shape Axis tree (first presented in Luh and Geifer [12]) and use an optimization function to find self-similarity in shapes. They identify the best match between two spline curves, one representing the parameterized shape and the other representing the shape parameterized in reverse. Gal et al. [5] present a new pose-oblivious shape signature function that defines the overall topography of a shape. This is achieved through use of the local diameter function and the centricity function Mademlis et al. [13] describe a method for shape retrieval by matching shapes with those in a database. The algorithm segments the shapes, and builds a probability matrix for each segment of each shaping, defining the probability that shape i in one shape matches shape j in the other. By applying a metric to this probability matrix, they determine the likelihood that the two shapes match.

These methods provide a useful basis for comparing two meshes, including height fields. However, our needs revolve around specific aspects of the terrains, namely the channel network. To the best of our knowledge, no shape analysis tools have been specifically applied to height field data in computer science literature. The closest approximation is the Hausdorff distance used to compare images ([8], [7], [11]). In our work, we use variations on the Hausdorff distance, as well as direct pixel to pixel comparisons, to determine the distance between two channel networks, a vital process for terrain comparison and failure diagnosis.

1.3 Contributions

Our framework consists of several analysis modules and distance metrics necessary for determining the important characteristics of a terrain and the distance between two terrains. Our contributions are:

1. An application of three shape difference metrics to measure distances between two extracted channel networks.

2. A method for determining an *ideal* flow threshold with which to extract the desired channel network.
3. A method for extraction of the important channel network of an eroded terrain through comparison with sequential neighbors.
4. The concept of a terrain's *fingerprint* and method for determining it, allowing for the comparison of terrains based on defining characteristics, such as number of channels, watershed width and depth, channel width and depth, eroded volume lost, channel meander, junction pixel balance, and pixel load.

2. TERRAIN ANALYSIS

In this section, we describe our method for determining the most appropriate flow threshold value for each terrain in a sequence. As input, our system takes in a series of chronologically sequential DEMs of a terrain surface, each at a different time during an erosion event. We wish to identify a flow threshold that produces similar enough channel networks on each terrain so that the generated terrain fingerprints are comparable.

For each pair of terrains D_{t_1} and D_{t_2} from a sequence, we compute the accumulated flow field and flow direction field, assigning a value to each pixel (grid space). We have developed an algorithm for determining the threshold τ for comparison between D_{t_1} and D_{t_2} . This algorithm averages a series of difference metrics that compute a value for the distance between two terrains' channel networks, and chooses the value for τ that minimizes this average. We have chosen to use variations of the Hausdorff distance, as well as a direct pixel-to-pixel comparison of the networks, to acquire a value for the distance. For our purposes, the most important measurement of distance between terrains is a measure of similarity between channel networks, and thus these metrics (limited to the pixels in the channel network) are chosen because they compare only the pixels in the network. Once τ is found, we visually compare the resulting channel networks for validation.

2.1 Channel Network Extraction

Once the flow direction field and flow field have been calculated for a terrain D , we can define its channel network based on a given threshold τ , designated N_τ . The flow of each pixel whose value is below τ is set to 0. Those pixels with positive flow remaining are assigned a designation. A pixel can be designated with one of four categorizations based on the flow direction of it and any of its eight neighbors that also reside in the extracted channel network:

- Channel Start (S): All non-zero neighbor pixels carry flow *away* from this pixel.
- Channel End (E): All non-zero neighbor pixels carry flow *into* this pixel. At least one neighbor must be non-zero.
- Channel Junction (J): Flows to exactly one neighbor, while more than one neighbor contributes to this pixel's flow.
- Channel (R): Exactly one neighbor contributes to the pixel's flow, and this pixel contributes to exactly one neighbor's flow.

It is important to note that, when using a flow accumulation algorithm in which a pixel's entire flow is applied to a single

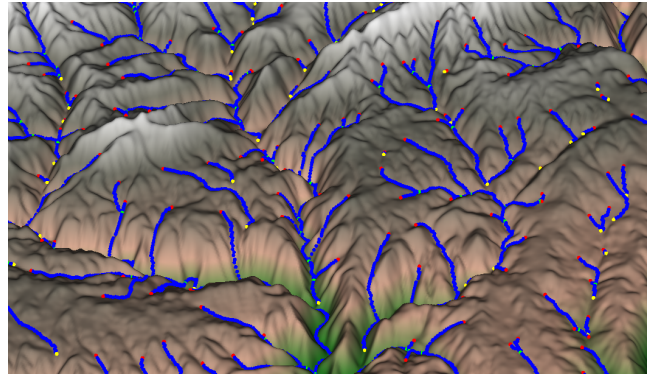


Figure 1: The segments and nodes that compose each channel network on the terrain are consistently labeled, starting from each channel end.

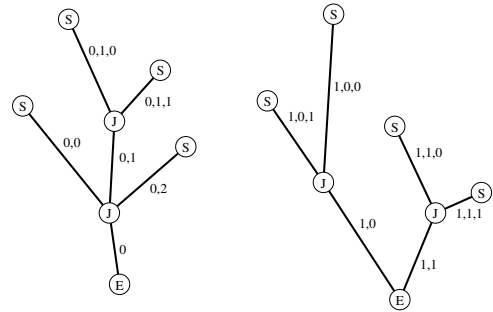


Figure 2: The segments and nodes that compose each channel network on the terrain are consistently labeled, starting from each channel end.

neighbor (as opposed to using a fractional flow method), channels can not split. An example of a channel network with designated start, end, and junction points is found in figure 1.

We define a channel *segment* as a set of pixels connecting an S to an E, an S to a J, a J to a J, or a J to an E. Segments will consist of exactly two S, E, or J pixels and a series of 0 or more 8-connected contiguous R pixels. We define a channel *network* as a series of connected segments. Each network can contain any number of S pixels but exactly one E pixel.

To each network within a terrain we assign an i.d. i , so a network in D is N_τ^i . To each pixel \mathbf{p} in N_τ^i we assign an *address*, designating in which N_τ^i it is found. The process of assigning addresses to pixels is a recursive tree traversal algorithm that begins at an E pixel and adds another level to the address whenever a J pixel is encountered, ending at an S pixel. An illustration of this addressing scheme is found in Figure 2.

2.2 Channel Network Metrics

We define three metrics that take as input two channel networks (N_τ^i and N_τ^j) and return the distance between them. These metrics are used to help define the difference between the terrains and thresholds from which the networks result. Since the metrics work with any channel networks, comparisons between terrains in the same sequence, between terrains for different sequences, or even the same terrain with a different chosen threshold are possible. We use these metrics to determine the distance between two

networks extracted using different thresholds from different points in the same sequence.

The first is the *pixel to pixel correspondence* metric, in which each pixel of N_τ^i is compared to each in N_τ^j , and two pixels are said to correspond if their addresses have the same length (they are each the same depth in their respective networks), and their flow travels in the same direction. We do not compare addresses directly because of potential inconsistencies in the labeling scheme applied to two similar but not identical networks. A slight change in threshold can cause a new, very small network to form elsewhere in the terrain, and as a result the ID system for the networks (Figure 2) is not comparable between thresholds, only a pixel's position within its own network.

$$dist_{pix}(N_\tau^i, N_\tau^j) = \frac{|\{\mathbf{p}_i \mid \mathbf{p}_i \rightarrow \mathbf{p}_j\}|}{|N_\tau^i|} \quad (1)$$

where $\mathbf{p}_i \in N_\tau^i$ and $\mathbf{p}_j \in N_\tau^j$ is its corresponding pixel (same x, y coordinates in its respective terrain), and $|N_\tau^i|$ is the total number of pixels compared, a normalizing component.

The second metric is the *Hausdorff distance* metric, defined as follows:

$$dist_{hauss}(N_\tau^i, N_\tau^j) = \max \left\{ \sup_{\mathbf{p}_i \in N_\tau^i} \inf_{\mathbf{p}_j \in N_\tau^j} d(\mathbf{p}_i, \mathbf{p}_j), \sup_{\mathbf{p}_j \in N_\tau^j} \inf_{\mathbf{p}_i \in N_\tau^i} d(\mathbf{p}_i, \mathbf{p}_j) \right\} \quad (2)$$

where $d(\mathbf{p}_i, \mathbf{p}_j)$ is the Euclidean distance between pixels \mathbf{p}_i and \mathbf{p}_j . This metric has the capability of lending too much weight to outliers, however, and so we introduce a third metric, the *average Hausdorff distance* metric:

$$dist_{avg}(N_\tau^i, N_\tau^j) = \max \left\{ \frac{\inf_{\mathbf{p}_i \in N_\tau^i} d(\mathbf{p}_i, \mathbf{p}_j)}{|N_\tau^i|}, \frac{\inf_{\mathbf{p}_j \in N_\tau^j} d(\mathbf{p}_i, \mathbf{p}_j)}{|N_\tau^j|} \right\} \quad (3)$$

or the maximum value of the average of the infimum of the distances between the sets. This metric tends to give a much more realistic look at the channel networks' distances.

2.3 Finding the Optimal Flow Threshold

If two adjacent terrains in a sequence produce channel networks that vary widely from one another, analyzing and comparing the terrains becomes more difficult. It is therefore beneficial to maintain temporal coherence for channel network extraction on a sequence. We introduce a moving window algorithm that uses the metrics introduced in section 2.2 to determine, for each terrain D_t , the threshold that minimizes its distance from its temporal neighbors.

```

avg ← 0
nComparisons ← 0
for wcur = t - WINDOW → t + WINDOW do
  for τ = τmin → τmax do
    dist ← d(Nτt, Nτwcur)
    avg ← avg + dist * c(dist)
    nComparisons ← nComparisons + 1
  end for
end for
avg ← avg/nComparisons

```

where $WINDOW$ is a constant window size, $d(N_\tau^t, N_\tau^{w_{cur}})$ is the distance between channel networks N_τ^t and $N_\tau^{w_{cur}}$,

$[\tau_{min}, \tau_{max}]$ is the range of threshold values we wish to test, and $c(dist)$ is a weight applied to the distance between networks. For our trials, a window size of 2 worked well for a 10-terrain sequence. For c , a weight of 1 is often sufficient.

3. RESULTS AND DISCUSSION

3.1 Data Collection

We collected data for our tests using the hydraulic erosion simulation presented by Chen et al. [4]. The simulation takes as input the geometry of a levee. Smoothed Particle Hydrodynamics (SPH) is used for both the fluid and erosion simulations, as the soil and water are both modeled with particles that have mass and volume. The level of erosion is based on the *erodibility* of the soil, which is a measure of the resistance of soil to the shear stress applied to it by flowing water. Once the critical shear stress is surpassed, erosion occurs, and water particles pick up soil particles to carry away. The output of the erosion simulation is a collection of particles. From these particles, we built a 200 x 200 DEM by ignoring all fluid particles and instead fitting a surface to the particles along the top of the terrain.

We identified water flow rate, geometry of the levee surface, and erodibility of the soil as three major simulation parameters influencing the progression of channel formation. This decision was a consequence of laboratory experiments in which the channel formation and time of breach were sensitive to changes to these parameters. We ran 27 simulations in total, including every combination of three different flow rates (slow, moderate, and fast), three levee down-slope angles (1:4, 1:5, and 1:6), and three erodibility values (minimally erodible clay, erodible sand-clay mix, and highly erodible sand). Full-scale levees are often built with a slope of 1:5. Taking a snap shot each minute for each ten minute simulation allotted us a large database from which to pull terrains and terrain sequences.

3.2 Comparison of Metrics

The most popular method for comparing terrain surfaces is a simple Root Mean Squares Error (RMSE) metric, which measures the root of the average squared difference in heights across the terrain (equation 4).

$$\sqrt{\frac{\sum_{\mathbf{p} \in D_{t_i}, \mathbf{q} \in D_{t_0}} (\mathbf{p}_z - \mathbf{q}_z)^2}{|D_{t_i}|}} \quad (4)$$

RMSE is most informative when measuring the difference between two terrains that should be identical, such as measuring the error introduced by a compression scheme. However, RMSE ignores the most important characteristic of a terrain, the channel network. We investigated how the error measurement changed when comparing sequential terrains. We looked at time steps from a 10-minute simulation from our set of 27 data points discussed in section 3.1 with typical results. The data sets can be seen in figure 3. We examined the change in error when comparing two time steps, t_1 and t_2 , using the first minute after t_1 as a baseline for comparison. The results can be seen in table 1.

The table shows the percent change of the value of the error with respect to the first minute of change for four time steps of the simulation, 0:00, 1:00, 5:00, and 9:00. As can be

t_1	t_2	$dist_{avg}$	% Δ	$dist_{RMS}$	% Δ
0:00	1:00	0.388953	N/A	0.000303	N/A
0:00	5:00	0.396261	0.0187884	0.014392	46.5655
0:00	9:00	0.405480	0.0424904	0.029450	96.3318
1:00	2:00	0.391023	N/A	0.002551	N/A
1:00	5:00	0.398034	0.0179307	0.014180	4.55904
1:00	9:00	0.407861	0.0430640	0.029254	10.4682
5:00	6:00	0.352744	N/A	0.004971	N/A
5:00	9:00	0.355777	0.0085981	0.018714	2.76438

Table 1: A table of the % change in average Hausdorff and RMSE distances for various time steps (t_i) of our erosion simulation with respect to the first minute after t_1 (the rows with “N/A” entries). We can see from this data that RMSE grows considerably as channels are dug (as time moves forward), whereas the average Hausdorff change is considerably smaller.

seen from the table, the RMSE value grows very quickly, as channels are dug deeper and the overall change in the terrain elevations is large. However, the average Hausdorff distance values grow much slower. What is more interesting is that, between times 1:00 and 9:00, the Hausdorff distance grows 0.0431%, but between 5:00 and 9:00 it increases 0.0086%, which is not proportional to the change from 1:00 to 9:00. The reason for this can be seen in figure 3, as channels had not formed yet as of early time steps (in the figure, time step 3:00), but by 5:00 they had. Since $dist_{avg}$ only takes into account pixels within the channel network, once it is formed, the distance between sequential terrains should be small. This data supports that hypothesis.

3.3 Thresholds With Temporal Coherence

For our trials, we tested thresholds between 20 and 1000 (about 0.1% to 0.05% of the maximum accumulated flow) with a change of discrete step of 20 units of flow per trial and a window size of 2. Figure 3 presents the results of our algorithm over the sequence of frames for the simulation of highly erodible soil with medium flow water on a 1:5 slope. We used an average of our three distance metrics to produce the target threshold.

Overall, the channel networks extracted behave as expected while maintaining a large degree of temporal coherence. As channels form along the downslope of the levee (facing the camera), our extracted channels change, split, and merge. Our simulation implements a small area sink in the middle of flat area at the foot of the levee, and thus, generally channels develop flowing into the sink. As the channels flowing to the sink grow, they consume and merge with the smaller channels on either side. Toward the early part of the simulation, there are several junction points located near the sink, but as the simulation progresses these merge into a single point. This behavior is consistent with the changing geometry of the levee in this area.

4. CONCLUSION AND FUTURE WORK

We have presented the *pixel correspondence* metric, the *Hausdorff distance* metric, and the *average Hausdorff distance* metric, each of which measure the difference between two extracted channel networks from an eroded terrain. Using them in conjunction with one another, we created an algorithm that uses a temporal window to take into account

the coherence with neighboring terrains in order to better decide on an ideal threshold to use when extracting a river network. We demonstrate that this method produces visually pleasing channel networks.

Our method is limited by the nature of our windowing algorithm. Possible thresholds are tested across neighbors, but the temporal coherence may be adversely affected by the neighbors’ choice for its threshold. In the future, we will consider an adaptive threshold, and allow each terrain to influence its neighbors’ choice of threshold. In our work, we use a static global threshold for each terrain. Better thresholding methods exist, such as watershed area dependant and elevation dependant methods. In the future, we will incorporate these more accurate definitions for a terrain’s threshold. Finally, the next natural step for our work is to build comparison techniques for terrain fingerprints. In order to accurately analyze them, independent component analysis will be utilized.

In addition, we will introduce the idea of a terrain fingerprint, a set of characteristics displayed by the terrain that are drawn from, and include, the hydrological channel network, or drainage network, that can be extracted from the terrain as described in section 2.1. Fingerprints are an important tool in forensic analysis of erosion, as they describe the evolution of the terrain under erosion. Once the terrain’s channel network is identified, a series of statistical and geometric characteristics are extracted, making up the terrain’s fingerprint. These characteristics describe a variety of aspects of the terrain including channel shape, drainage density, flow pattern, and individual pixel importance. A fingerprint provides a description of a terrain surface. One important application is the determination of a measure of dissimilarity between two terrains by assigning a quantity to the distance between their fingerprints, similar to the terrain metrics described in this paper. Future work includes development of the fingerprint and its application to distance metrics for terrain comparison.

Acknowledgments

This research was partially supported by NSF grants CMMI-0835762 and IIS-1117277.

5. REFERENCES

- [1] L. Band. Topographic partition of watersheds with digital elevation models. *Water Resources Research*, 22(1):15–24, January 1986.
- [2] S. Belongie, J. Malik, and J. Puzicha. Shape Context: A new descriptor for shape matching and object recognition. In *In NIPS*, pages 831–837, 2000.
- [3] S. Belongie, J. Malik, and J. Puzicha. Shape matching and object recognition using shape contexts. *IEEE Trans. Pattern Anal. Mach. Intell.*, 24:509–522, April 2002.
- [4] Z. Chen, C. S. Stuetzle, B. M. Cutler, J. A. Gross, W. R. Franklin, and T. F. Zimmie. Analyses, simulations and physical modeling validation of levee and embankment erosion. In *Geo Frontiers 2011*, Dallas, Texas, US, 2011.
- [5] R. Gal, A. Shamir, and D. Cohen-Or. Pose-oblivious shape signature. *IEEE Transactions on Visualization and Computer Graphics*, 13(2):261–271, 2007.

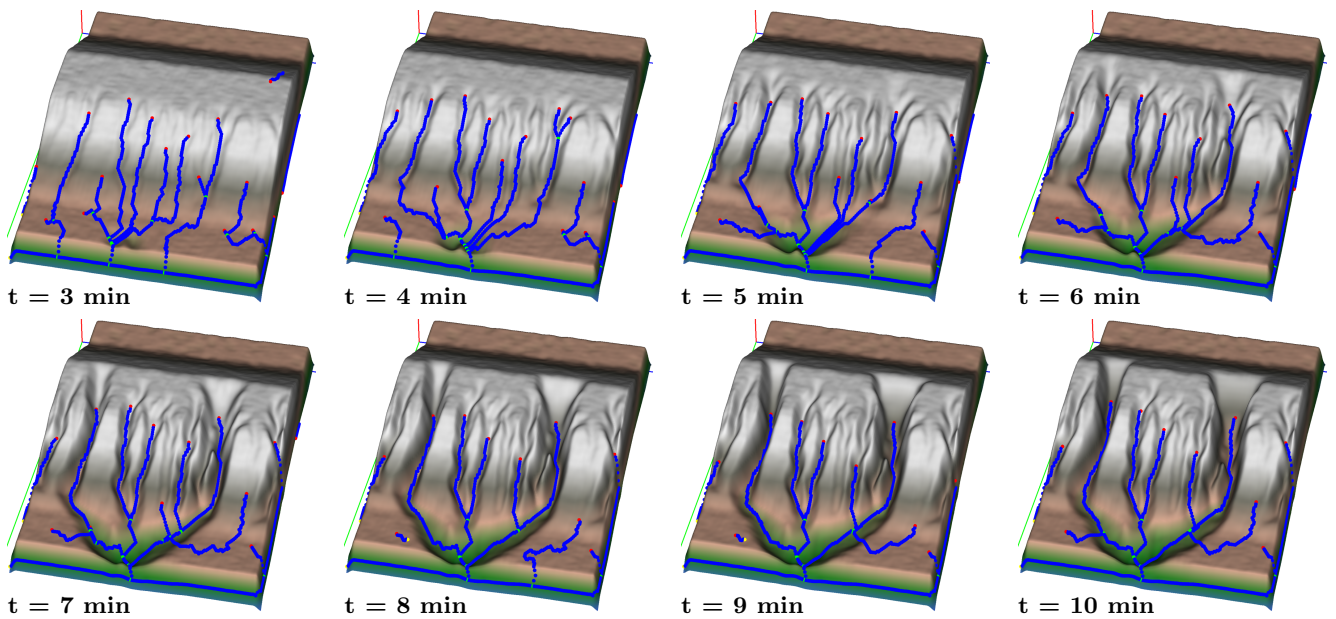


Figure 3: The channel networks in these images were extracted using our thresholding algorithm. The extracted networks mimic the behavior of the geometry while maintaining temporal coherence.

- [6] D. Geiger, T.-L. Liu, and R. V. Kohn. Representation and self-similarity of shapes. *IEEE Trans. Pattern Anal. Mach. Intell.*, 25:86–99, January 2003.
- [7] D. P. Huttenlocher, G. A. Klanderman, and W. A. Rucklidge. Comparing images using the hausdorff distance. *IEEE Trans. Pattern Anal. Mach. Intell.*, 15:850–863, September 1993.
- [8] O. Jesorsky, K. J. Kirchberg, and R. W. Frischholz. Robust Face Detection Using the Hausdorff Distance. In J. Bigun and F. Smeraldi, editors, *Audio- and Video-Based Person Authentication - AVBPA 2001*, volume 2091 of *Lecture Notes in Computer Science*, pages 90–95, Halmstad, Sweden, 2001. Springer.
- [9] S. Kramer and M. Marder. Evolution of river networks. *Phys. Rev. Lett.*, 68(2):205–208, Jan 1992.
- [10] B. Lashermes, E. Foufoula-Georgiou, and W. E. Dietrich. Channel network extraction from high resolution topography using wavelets. *Geophysical Research Letters*, 34(23):L23S04+, Oct. 2007.
- [11] R. Lipikorn, A. Shimizu, and H. Kobatake. A modified exoskeleton and a hausdorff distance matching algorithm for shape-based object recognition. In *CISST'03*, pages 507–511, 2003.
- [12] T.-L. Liu and D. Geiger. Approximate tree matching and shape similarity. In *Computer Vision, 1999. The Proceedings of the Seventh IEEE International Conference on*, volume 1, pages 456–462 vol.1, 1999.
- [13] A. Mademlis, P. Daras, A. Axenopoulos, D. Tzovaras, and M. G. Strintzis. Combining topological and geometrical features for global and partial 3-d shape retrieval. *IEEE Transactions on Multimedia*, 10:819–831, 2008.
- [14] M. Metz, H. Mitasova, and R. S. Harmon. Efficient extraction of drainage networks from massive, radar-based elevation models with least cost path search. *Hydrology and Earth System Sciences*, 15(2):667–678, 2011.
- [15] D. R. Montgomery. Channel network source representation using digital elevation models. *Water Resources Research*, 29(12):3925–3934, December 1993.
- [16] J. F. O’Callaghan and D. M. Mark. The extraction of drainage networks from digital elevation data. *Computer Vision, Graphics, and Image Processing*, pages 323–344, 1984.
- [17] R. Osada, T. Funkhouser, B. Chazelle, and D. Dobkin. Shape distributions. *ACM Transactions on Graphics*, 21(4):807–832, Oct. 2002.
- [18] M. Roy, S. Foufou, and F. Truchetet. Mesh comparison using attribute deviation metric. *Journal of Image and Graphics*, 4:1–14, 2004.
- [19] R. Seed, P. Nicholson, R. Dalrymple, J. Battjes, R. Bea, G. Boutwell, J. Bray, B. D. Collins, L. Harder, J. Headland, M. Inamine, R. Kayen, R. Kuhr, J. M. Pestana, R. Sanders, F. Silva-Tulla, R. Storesund, S. Tanaka, J. Wartman, T. F. Wolff, L. Wooten, and T. Zimmie. Preliminary Report on the Performance of the New Orleans Levee Systems in Hurricane Katrina, August 2005.
- [20] P. Soille, J. Vogt, and R. Colombo. Carving and adaptive drainage enforcement of grid digital elevation models. *Water Resources Research*, 39, 2003.
- [21] R. Turcotte, J. Fortin, A. Rousseau, S. Massicotte, and J. Villeneuve. Determination of the drainage structure of a watershed using a digital elevation model and a digital river and lake network. *Journal of Hydrology*, 240(3-4):225–242, 2001.
- [22] D. Yang, S. Herath, and K. Musiak. Analysis of geomorphologic properties extracted from dems for hydrologic modeling. *Annual Journal of Hydraulic Engineering*, 41, 1997.